Pure Appl. Geophys.

DOI 10.1007/s00024-014-1008-3

Pure and Applied Geophysics

Landslide Kinematical Analysis through Inverse Numerical Modelling and Differential SAR Interferometry

R. Castaldo,[1] P. Tizzani,[1] P. Lollino,[3] F. Calò,[1] F. Ardizzone,[2] R. Lanari,[1] F. Guzzetti,[2] and M. Manunta[1]

Abstract—The aim of this paper is to propose a methodology to perform inverse numerical modelling of slow landslides that combines the potentialities of both numerical approaches and well-known remote-sensing satellite techniques. In particular, through an optimization procedure based on a genetic algorithm, we minimize, with respect to a proper penalty function, the difference between the modelled displacement field and differential synthetic aperture radar interferometry (DInSAR) deformation time series. The proposed methodology allows us to automatically search for the physical parameters that characterize the landslide behaviour. To validate the presented approach, we focus our analysis on the slow Ivancich landslide (Assisi, central Italy). The kinematical evolution of the unstable slope is investigated via long-term DInSAR analysis, by exploiting about 20 years of ERS-1/2 and ENVISAT satellite acquisitions. The landslide is driven by the presence of a shear band, whose behaviour is simulated through a two-dimensional time-dependent finite element model, in two different physical scenarios, i.e. Newtonian viscous flow and a deviatoric creep model. Comparison between the model results and DInSAR measurements reveals that the deviatoric creep model is more suitable to describe the kinematical evolution of the landslide. This finding is also confirmed by comparing the model results with the available independent inclinometer measurements. Our analysis emphasizes that integration of different data, within inverse numerical models, allows deep investigation of the kinematical behaviour of slow active landslides and discrimination of the driving forces that govern their deformation processes.

Key words: Numerical modelling, optimization procedure, differential SAR interferometry, slow landslide.

1. Introduction

Management of risk associated with slow-moving active landslides requires analysis of the kinematical evolution of the unstable mass in terms of displacements, velocity or acceleration over time (Alonso 2012; Ledesma *et al*. 2009), more than the assessment of the stability conditions of the landslide mass, which instead refer to static conditions, such as those corresponding to the triggering or reactivation stages. Indeed, study of the kinematical trend of a landslide represents an effective way for predicting, and therefore mitigating, the eventual damage caused by landslide movements to buildings and infrastructures.

In this framework, numerical modelling allows simulation of the stress–strain state of a landslide process during both the triggering and propagation stages, provided that a suitable modelling approach is pursued and the factors controlling the landslide evolution are correctly implemented in the model, along with the geological and geotechnical information available for the examined slope (Troncone 2005; Lollino *et al*. 2011).

However, when the objective of the numerical analysis is time-dependent simulation of the kinematical evolution of complex phenomena, such as the case of mass movements, a critical role is represented by the selection of a proper physical approach, suitable to correctly describe the investigated phenomenon. In this context, several works have focussed on studying and predicting the time-dependent law of variation of the displacement pattern of slow active landslides (Vulliet and Hutter 1988; Ledesma *et al*. 2009; Crosta *et al*. 2012). In particular, soil viscosity or changes in the slope boundary conditions play a remarkable role as leading factors controlling the landslide dynamics, and should be properly accounted for in the simulation of the landslide evolution. For slopes characterized by deformation patterns that are weakly affected by

[1] CNR IREA, via Diocleziano 328, 80127 Naples, Italy. E-mail: castaldo.r@irea.cnr.it
[2] CNR IRPI, via della Madonna Alta 126, 06128 Perugia, Italy.
[3] CNR IRPI, via Amendola 122 I, 70126 Bari, Italy.

Published online: 23 December 2014

changes in the hydraulic boundary conditions, namely characterized by a steady-state pore water pressure regime, adequate viscous-type sliding laws should be assumed to simulate the slope displacement trends of the involved soils (Vulliet and Hutter 1988, Leroueil 2001; Pastor *et al*. 2002). In this case, several constitutive approaches are available in the literature to reproduce creep displacement patterns in time-dependent numerical models (Pastor *et al*. 2002), ranging from simulation of soils in terms of Newtonian or non-Newtonian fluids, to the assumption of visco-plastic behaviour of the soil according to a Bingham fluid (Perzyna 1966; Vulliet and Hutter 1988; Crosta *et al*. 2012) or more advanced visco-plastic fluid approaches (Chen and Ling 1996). In particular, following earlier experimental results from Bagnold (1954) and more recent work from Hunt *et al*. (2002), the behaviour of a dispersion of granular particles in a viscous fluid at low strain rates, e.g. in the macro-viscous region where viscosity effects are dominant, can be effectively reproduced by means of a Newtonian fluid model. This approach accounts for a linear relationship between the shear stress and strain rate of the material according to a viscosity parameter that depends on the solid particle concentration. Regarding the behaviour of mudflows and flow-slides, Pastor *et al*. (2002) state that, after the landslide initiation stage, the soil material under shear behaviour can be considered as subjected to fluidification, and as a consequence, the behaviour of fluidised mixtures of soil and water can be described by rheological laws relating total shear stresses to strain rates. The same authors also highlight that such a total stress approach is mostly valid in extreme cases where the permeability of the soil is very low and pore pressures do not change significantly during the sliding process.

Despite such advancements in the field, the search for proper values of the parameters associated with the physical approach adopted to simulate landslide kinematical evolution remains a critical stage due to the lack of methodologies and procedures capable of efficiently calibrating forward numerical models. An efficient way to overcome this limitation is exploitation of inverse numerical optimization algorithms aimed at estimating the correct values of kinematical parameters. The use of inverse numerical modelling approaches has already been proposed in other geoscience fields, such as seismology and volcanology (Tizzani *et al*. 2010, 2013), where they are applied to extract a synoptic view of the investigated natural events.

In this work, we propose a new methodology to properly perform inverse numerical modelling of landslides. The developed procedure is based on the integration of geological, geomorphological, geotechnical and geodetic information. In particular, we exploit satellite differential synthetic aperture radar interferometry (DInSAR) techniques that are proving to be a valuable tool for long-term deformation monitoring of slow-moving landslides and can provide useful information for predicting landslide kinematical evolution, assuming that the slope boundary conditions do not change over time (Hilley *et al*. 2004; Farina *et al*. 2006; Guzzetti *et al*. 2009; Cascini *et al*. 2009, 2010; Calò *et al*. 2012). In our methodology, DInSAR deformation time series are effectively used to calibrate the numerical model through an optimization procedure that minimizes, with respect to a proper cost function, the difference between the modelled displacement field and the DInSAR measurements. A preliminary example of the application of inverse numerical modelling methods to landslide scenarios has already been proposed in Calò *et al*. (2014), developed by exploiting mean deformation velocity DInSAR maps. In this work, we present a detailed analysis of the proposed methodology, based on the exploitation of long-term deformation time series.

As a representative case study, maintaining continuity with previous work, the Ivancich landslide (Assisi, central Italy) is considered. This landslide affects a slope formed of pelitic sandstone, and is characterized by a sliding surface at depths ranging from 15 to 60 m from the ground surface. The landslide displacement rate is around 1 cm/year at maximum, and the corresponding trends are observed to be quite independent of water table fluctuations or pore water pressure variations at the depth of the sliding surface. It appears that the landslide process seems to be controlled more by viscous factors than by changes in the hydraulic boundary conditions. Accordingly, the soil flowing within the thin shear zone of the Ivancich landslide is simulated through two different physical approaches, i.e. Newtonian fluid dynamics and a deviatoric creep model. We perform two-dimensional finite-element (FE) analysis aimed at calculating the kinematics of the landslide mass in the recent evolution stage, by investigating the behaviour of the soil characterizing the thin shear band. The numerical results are calibrated through DInSAR deformation time series covering nearly 20 years (1992–2010) and then are validated by means of independent inclinometer measurements performed in four boreholes located along the slope.

Our results clearly demonstrate that integration of advanced numerical modelling approaches and satellite remote sensing monitoring techniques results in a tool suitable for study of the behaviour of the Ivancich landslide and, more generally, analysis of the kinematical evolution of slow landslides characterized by similar geological and mechanical features.

2. *Numerical Analysis and Optimization Procedure*

Ground deformations are the expression of near-surface and/or deep-seated geological processes. In the earth science context, interpretation of deformation measurements can be effectively performed by setting up inverse problems to constrain the nature of the causative factors and the values of representative parameters. Numerical methods based on inverse analysis exploit the problem's solution space by iterating a large set of forward mathematical models, which instead can be affected by uncertainty as regards specific parameters or problems of oversimplification in model construction.

In this perspective, inverse models based on the FE method are a suitable tool to fill the gap between the accuracy achieved in the field of ground deformation observations and the models used for the corresponding interpretation. For this reason, we propose a numerical approach based on inverse FE models that are constrained by field and DInSAR-based monitoring data as an alternative to standard forward FE models (Tizzani *et al*. 2010, 2013). In particular, we combine the benefits of the numerical approach with a Monte Carlo optimization procedure referred to as a genetic algorithm (GA) (Gill *et al*. 1981; Bingul *et al*. 2000), to analyse and interpret ground deformations measured in active landslide areas. The GA optimization approach derives from the theory of biological evolution. By analogy, the algorithm starts with an initial set of models (population) randomly generated by imposing as input data to the procedure parameter values ranging within appropriate intervals. Within this population, the best solution, defined as the set of parameter values providing the best fit between the numerical solution and the landslide behaviour as observed by available monitoring data, is found through minimization of a defined cost function. Numerical operators for mutation and chromosome crossover (recombination) act on the best individuals, resulting in the breeding of a new population of "evolved" individuals; i.e. only models that survived the preceding selection may reproduce and proceed to the next step (generation). According to Manconi *et al*. (2009), the procedure is thus iterated until reaching a previously assigned maximum number of generations. The optimization procedure performed in the present analysis is based on minimization of the discrepancy between DInSAR data and the results of the FE model in terms of the calculated displacement rate. In our study, the cost function is based on the root-mean-square error (RMSE) between the modelled and observed data.

To investigate the kinematical evolution of a landslide, various physical approaches can be considered according to the characteristics of the analysed phenomenon. In our case, we focussed on two physical approaches, i.e. the Newtonian and deviatoric creep models, which are suitable to simulate the kinematical trend of the Ivancich landslide, selected as a test site for the proposed methodology. In particular, the former approach consists in the application, within a fluid dynamics context (i.e. solving for the velocity using the Navier–Stokes equations), of a Newtonian viscosity model for which the stress distribution and velocity field are governed by the dynamic viscosity. In the latter approach, the temporal evolution of the ground deformation field is assumed to be governed by the soil creep rate distribution, and accordingly, the role of the secondary creep behaviour in a structural mechanical context (i.e. solving for the displacements using the Navier equations) is investigated. As a tool to integrate all the available data and solve the considered equations in both physical approaches, we use the COMSOL Multiphysics finite-element modeling code (http://www.comsol.com/).

2.1. Fluid Dynamics Model

For active landslides characterized by a quasi-linear displacement trend, the kinematical evolution can be described through a numerical model based on the approximation of the material behaviour as a Newtonian fluid characterized by a viscosity constant over time. Accordingly, we can assume a steady-state viscous flow (Newtonian fluid) solved through the incompressible Navier–Stokes differential equations:

$$\begin{aligned} &-\nabla \cdot \eta\left(\nabla \mathbf{u} + (\nabla \mathbf{u})^T\right) + \rho(\mathbf{u} \cdot \nabla)\mathbf{u} + \nabla p = \mathbf{F} \\ &\nabla \cdot \mathbf{u} = \mathbf{0}, \end{aligned} \quad (1)$$

where $\mathbf{u}$ (m/s) is the deformation velocity vector, $\mathbf{F}$ (Pa/m) is the body force term, ρ (kg/m^3) is the density, p (Pa) is the pressure, and η is the dynamic viscosity (Pa s) (hereafter referred to as viscosity).

The viscosity distribution can be evaluated through an advanced procedure implementing non-linear optimization of the FE model with respect to the available displacement measurements. In our approach, we searched for the best-fit viscosity model explaining the observed DInSAR displacement rates. In particular, the model deformation velocities are calculated at the topographic surface, projected along the satellite line of sight (LOS), and compared with the DInSAR measurements. The best-fit viscosity model is finally selected by considering the minimum (RMSE) as the cost function.

2.2. Creep Model

When dealing with steady-state kinematical trends, as an alternative to the Newtonian fluid model, a deviatoric creep model characterized by a creep rate depending on the deviatoric component of the stress state can be chosen to simulate the behaviour of soil. This model is suitable to simulate soil material undergoing secondary creep (steady-state creep), with the creep rate almost constant over time and depending on the current stress level of the soil. In the inverse analysis, the creep rate can be adopted as the unknown parameter to be defined through the optimization procedure. In this physical scenario, the creep strain rate (ε_c) is calculated by solving the following equation:

$$\frac{\mathrm{d}\varepsilon_c}{\mathrm{d}t} = F_{cr} n^D, \quad (2)$$

where $\mathbf{n}^D$ is the deviatoric component of the stress tensor, and F_{cr} (1/s) represents the creep rate. The deviatoric tensor $\mathbf{n}^D$ is defined as follows:

$$n^D = \frac{3}{2} \frac{(\sigma_{11} - \sigma_{33})}{\begin{vmatrix} \sigma_{11}\sigma_{12}\sigma_{13} \\ \sigma_{21}\sigma_{22}\sigma_{23} \\ \sigma_{31}\sigma_{32}\sigma_{33} \end{vmatrix}}, \quad (3)$$

where σ_{11}, σ_{22} and σ_{33}, respectively, represent the maximum, intermediate and minimum principal stresses of the soil and $\sigma_{ij\ (i \neq j)}$ is the shear stress in the *i*–*j* plane. The creep rate F_{cr} normally depends on the second deviatoric invariant of the stress (in addition to the temperature and other material parameters), and the effective creep strain rate equals the absolute value of F_{cr}:

$$\frac{\mathrm{d}\varepsilon_{cc}}{\mathrm{d}t} = |F_{cr}|. \quad (4)$$

As for the fluid dynamics model case, the creep rate distribution is evaluated through an advanced procedure allowing for the application of non-linear optimization algorithms to FE models. In particular we search for the best-fit creep rate model with respect to the observed DInSAR deformation measurements.

3. Case Study: the Ivancich Landslide

For our study, we focussed on the Ivancich area, a neighbourhood located in the eastern part of the historical town of Assisi (central Italy), and affected by an active slow-moving landslide since its first urbanization (Antonini *et al.* 2002). Damage caused by slow movement of the landslide to buildings and infrastructure has led local authorities to carry out several geological and geotechnical investigations aimed at implementing effective remedial work and mitigation strategies (Felicioni *et al*. 1996; Angeli and Pontoni 2000, 2011). As a result, the area has been deeply investigated in the last 20 years and extensively monitored through in situ inclinometers and piezometers (Pontoni 1999, 2011; Fastellini *et al*. 2011). Geomorphological and topographic surveys revealed that the phenomenon is an old translational slide, with a rotational component in the source area, moving along a well-defined shear band (Cruden and Varnes 1996). In particular, the mass movement involves a debris deposit, from 15 to 60 m in thickness, overlaying a bedrock that consists of a pelitic sandstone unit and layered limestone (Fig. 1a, b) (Servizio Geologico Italiano 1980; Canuti *et al*. 1986; Angeli and Pontoni 2000; Cardinali *et al*. 2001).

3.1. Ground-Based Data

Several campaigns of sub-surface investigations, consisting of inclinometer and piezometer measurements, have been carried out in the Ivancich landslide area, aimed at defining the geometry of the sliding mass and acquiring data on sub-surface displacements and the groundwater regime. In particular, displacement–depth profiles collected between 1998 and 2009 in four inclinometer boreholes approximately located along the central longitudinal section of the landslide body (Fig. 1a, b) pointed out the existence of a shear zone characterized by thickness of less than 2 m, above which the landslide material moves nearly as a rigid body on the stable bedrock (Fig. 1c) (Angeli and Pontoni 2000; Pontoni 2011). The higher cumulated displacements at the ground surface were recorded in the middle portion of the unstable slope, where two inclinometers, namely inclinometers 113 and 117 in Fig. 1a, respectively detected about 7.5 cm between December 1998 and December 2005 and about 6 cm between December 1998 and July 2004 (Fig. 1c). Therefore, these data highlight the major activity of the mid-slope sector, which has been confirmed by DInSAR data (Sect. 3.2).

Regarding the groundwater regime, unpublished piezometer data acquired in the landslide deposit reveal that the pore water pressure affects the landslide kinematics quite moderately. In particular, the ground water surface was measured to be, in general, only a few metres above the shear band. This results in very low piezometric heights, when compared with the total stress levels. Also, the piezometric surface was observed to be approximately constant over time, with limited seasonal fluctuations. We can consider this a further indication of the limited influence of the rainfall pattern and of the slope groundwater regime on the landslide kinematics, which is characterized by displacement rates that are approximately constant in time over long periods (Calò *et al*. 2014).

3.2. DInSAR Data

For our purposes we benefited from the capability of the multi-sensor Small BAseline Subset (SBAS) approach (Bonano *et al*. 2012) to generate very long deformation time series exploitable for landslide back-analyses. In particular, such a technique, by jointly processing data acquired by geometrically compatible SAR sensors, as in the case of ERS-1/2 and ENVISAT acquisitions, allows production of deformation time series spanning a period of almost 20 years, with accuracy of about 5 mm (Calò *et al*. 2014).

In this work, we exploit the SBAS results, presented in Calò *et al*. (2014), achieved by processing a SAR dataset of 130 ERS-1/2 and ENVISAT images, acquired from 21 April 1992 to 12 November 2010 over central Umbria (Italy). Application of the SBAS DInSAR technique provided a ground deformation velocity map, and associated time series of displacements [measured along the satellite line of sight (LOS)], for the whole study area. The performed analysis allowed detection of a large number of SAR measurement points over the Ivancich landslide (Fig. 2a). For our back-analysis, we selected six SAR pixels located within a distance of 25 m from the landslide longitudinal section S–S′ (Fig. 2b, c).

4. Model Setup

To investigate the kinematical evolution of the Ivancich landslide, we carried out two-dimensional (2D) time-dependent FE modelling of the active

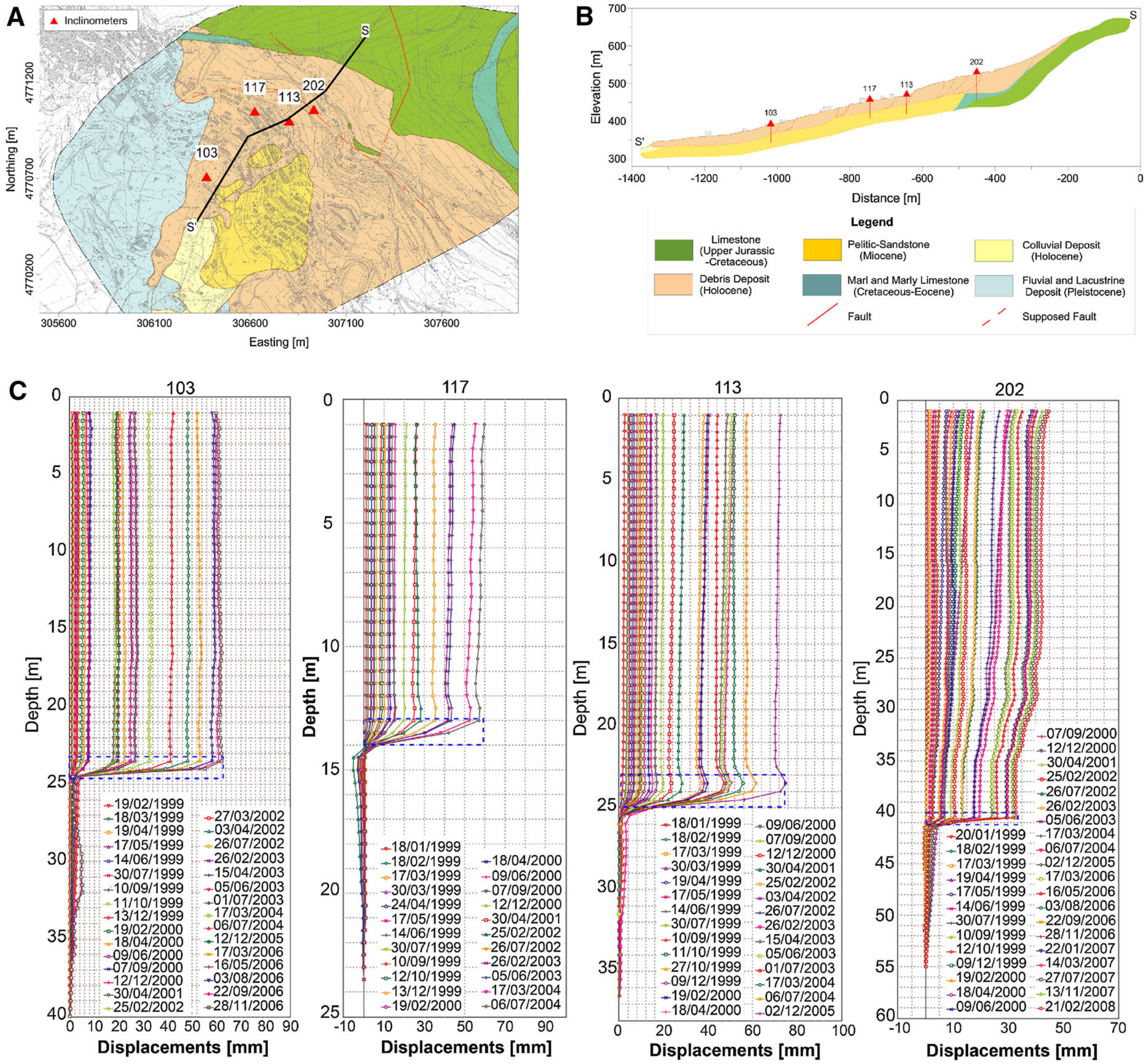

Figure 1

a Geological map of the study area superimposed on a topographic map (modified from Angeli and Pontoni 1999). The *black line* represents the trace of the geological section S–S′. *Red triangles* show locations of inclinometers. **b** Geological section S–S′, and location of inclinometers (*red triangles*). **c** Displacement–depth profiles for inclinometers 103, 117, 113 and 202. The *dotted rectangle* represents the depth and thickness of the shear band

ground deformation field using the fluid dynamics and deviatoric creep physical models described above.

We defined the mesh domain of the FE model by exploiting the available geological and geotechnical data obtained from previous investigation campaigns and sub-surface monitoring surveys (Angeli and Pontoni 2000). Based on such information, we set up the 2D model of the whole slope representing the S–S′ longitudinal section of Fig. 2b. In particular, as shown in Fig. 3a, we subdivided the discretization mesh into five geo-mechanical units (see Table 1 for physical properties): (1) a limestone bedrock, in the upper part of the slope, (2) a pelitic sandstone bedrock, in the central and lower portions of the slope, (3) the landslide deposit, formed of unsorted debris, (4) a colluvial deposit, in the landslide toe area, and (5) a shear zone, characterized by thickness of less

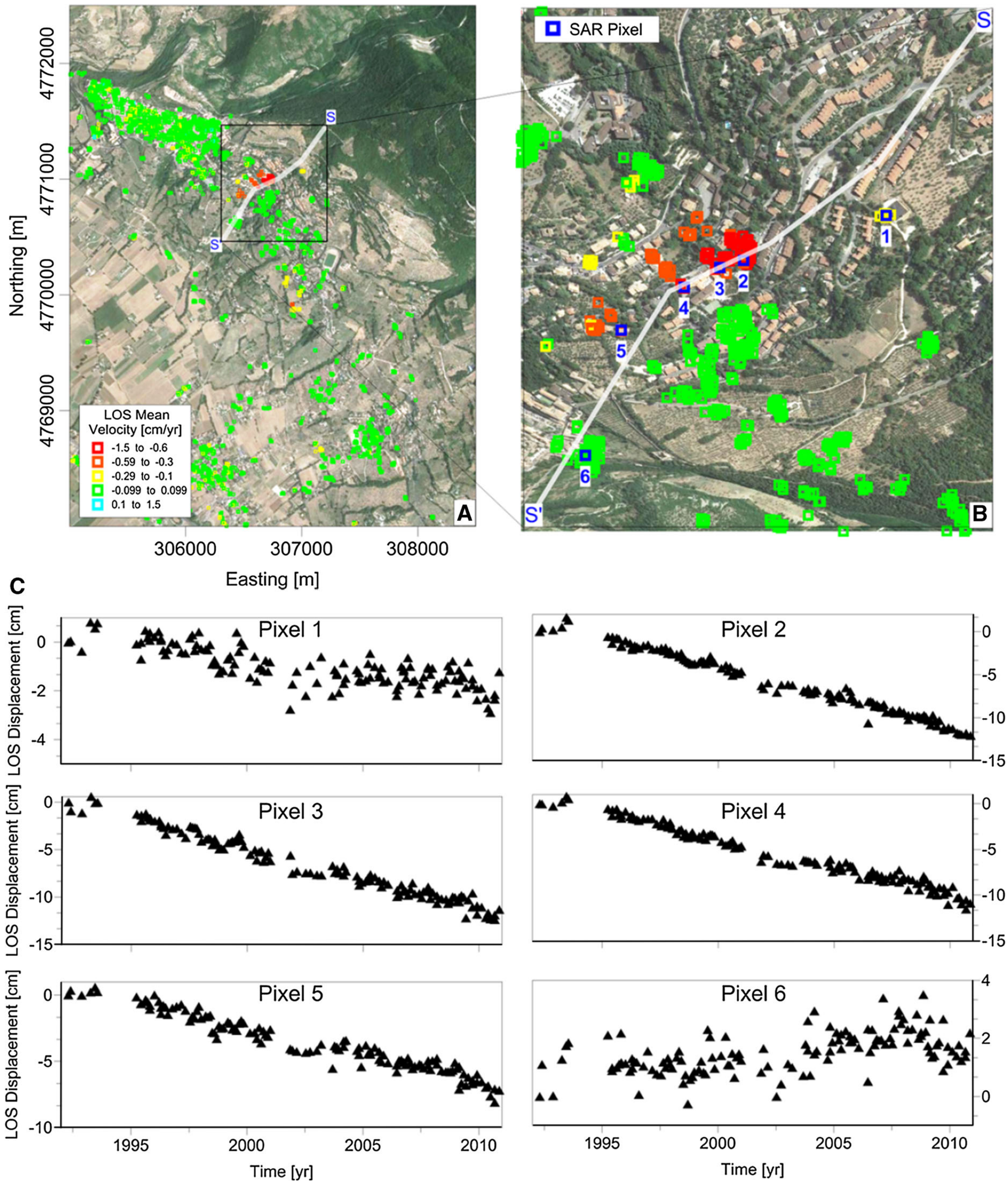

Figure 2

a Ground deformation velocity map obtained through SBAS DInSAR processing of descending ERS-1/2 and ENVISAT data, for Assisi (central Italy). *Inset* shows a zoom over the Ivancich landslide. **b** Zoom over the Ivancich landslide, and location of the six SAR pixels selected for analysis (*blue squares*). *White line* shows the geological section S–S′. **c** Deformation time series of the SAR pixels reported in **b**. Displacements measured along the satellite line of sight (LOS)

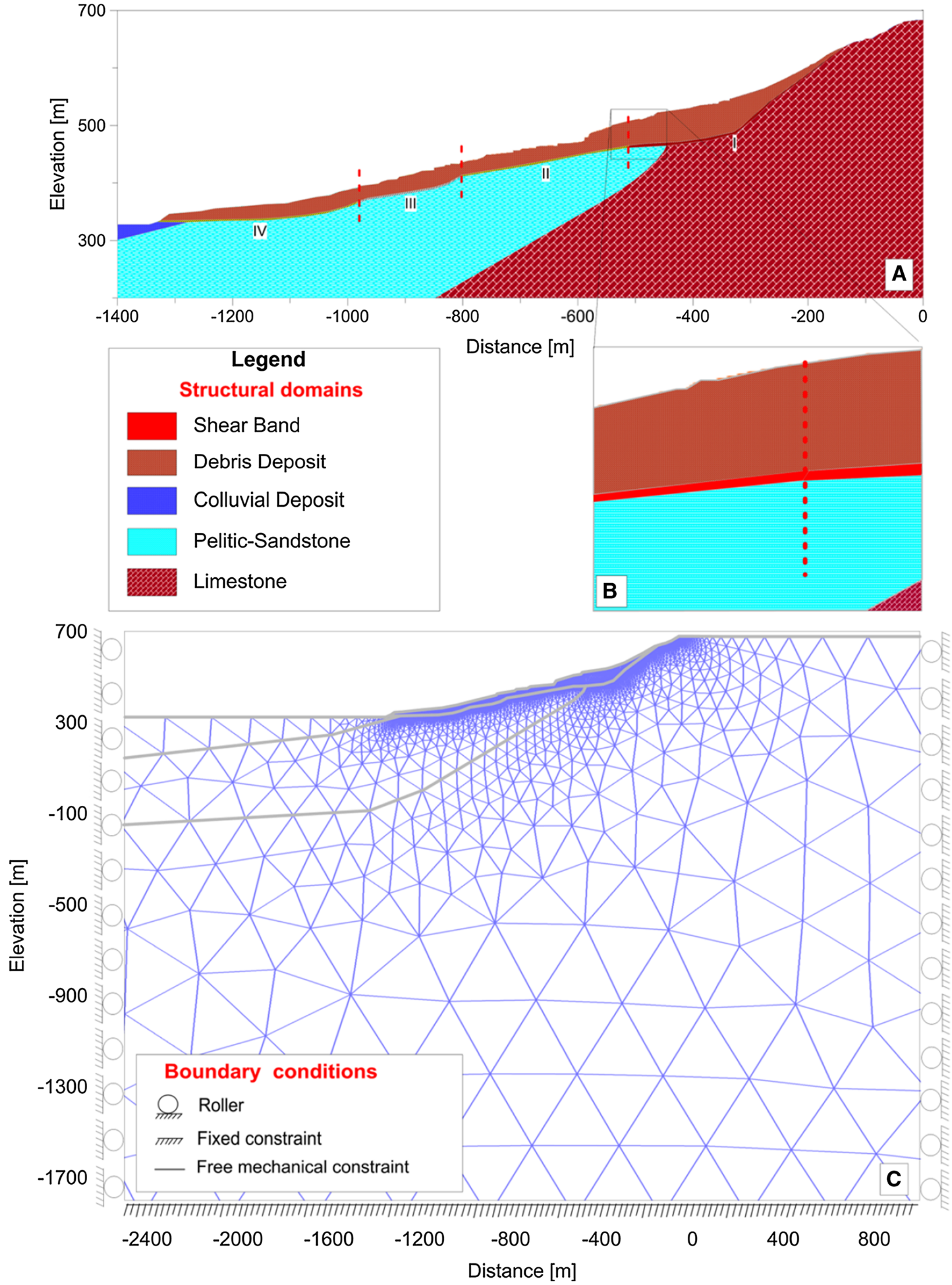

Figure 3
a Simplified 2D model geometry with structural domains. *Inset* **b** shows the shear band domain. **c** Boundary conditions and model geometry superimposed on the triangular FE mesh

Table 1

Physical properties used for different geo-mechanical units

Input parameters				
Rock material	Density (kg/m^3)	Young's modulus (MPa)	Poisson ratio (–)	Viscosity (Pa s)
Limestone bedrock	2,200	8×10^3	0.28	1×10^{20}
Pelitic sandstone bedrock	1,850	7×10^3	0.26	1×10^{19}
Debris deposit	1,600	1×10	0.24	1×10^{18}
Colluvial deposit	1,700	6×10	0.24	1×10^{18}
Shear band	1,600	1×10	0.23	–

Table 2

Physical parameter bounds used for the four shear band sectors within the optimization procedure and estimated values

Output parameters			
	Lower bound	Upper bound	Estimated value
Viscosity (Pa s)			
η_1	1×10^{14}	5×10^{16}	7×10^{15}
η_2	1×10^{13}	5×10^{15}	1.5×10^{14}
η_3	1×10^{13}	5×10^{15}	1×10^{14}
η_4	1×10^{14}	5×10^{16}	2.2×10^{15}
Creep rate (1/year)			
F_{cr1}	1×10^{-3}	5×10^{-5}	9×10^{-4}
F_{cr2}	1×10^{-2}	5×10^{-4}	8×10^{-3}
F_{cr3}	1×10^{-2}	5×10^{-4}	7×10^{-3}
F_{cr4}	1×10^{-3}	5×10^{-5}	3.5×10^{-4}

than 2 m, with depth ranging between 15 and 60 m from the ground surface (Pontoni 1999, 2000 and Angeli). According to Calò *et al.* (2014), the shear band domain was divided into four homogeneous sectors in order to comply with the evidence of corresponding inner landslide bodies, characterized by different slope angles, crests and toes, as detected by the available geological and geomorphological information. This evidence is also supported by the analysis of the DInSAR measurements, proving that the identified sectors are characterized by different kinematical rates. It is worth noting that this shear band domain subdivision has no significant impact on the general applicability of our approach, and a finer discretization, although involving an increase of the computational load, can be easily applied in more complex scenarios.

Note that, in the fluid dynamics scenario, for the geo-mechanical units neighboring the shear surface, the physical model input parameters (Table 1) include significantly high viscosity values (Renzhiglov and Pavlishcheva 1970) to simulate the much lower shear rates; this approach is in agreement with the available inclinometric data. On the other hand, for the deviatoric creep model analysis, we associate the creep rate parameters only with the shear band zone, to simulate its physical behaviour.

Regarding the boundary conditions, the upper part of the model, which represents the ground surface, is considered as unconstrained, whereas the bottom side is fixed in both the vertical and horizontal directions; the vertical side boundaries of the model are instead characterized by null horizontal displacement to make edge effects negligible. The inner domain is characterized by continuity between the different geological units.

Subsequently, we defined the mesh domain, discretized into about 22,000 triangular elements characterized by maximum and minimum sides of 400 and 5 m, respectively, and we applied mesh refinement along the shear band domain (Fig. 3b). The generated mesh was then validated through several resolution tests (Zienkiewicz and Taylor 1988; Zhang and Zhu 1998), which indicated that the use of a finer mesh would affect the results by less than 2 %.

Similarly to Griffiths and Lane (1999) and Tizzani *et al.* (2013), we performed our modelling in two stages, i.e. a first step of gravity loading aimed at defining a stress field representative of the current stress state of the slope, and a second step of landslide kinematics simulation.

During the first stage (gravity loading), the stress state of the slope is defined by considering the slope as subjected to the soil gravitational loads and assuming elastic soil behaviour; at this level, only the generated stress field is considered, while the nodal displacements are kept equal to zero.

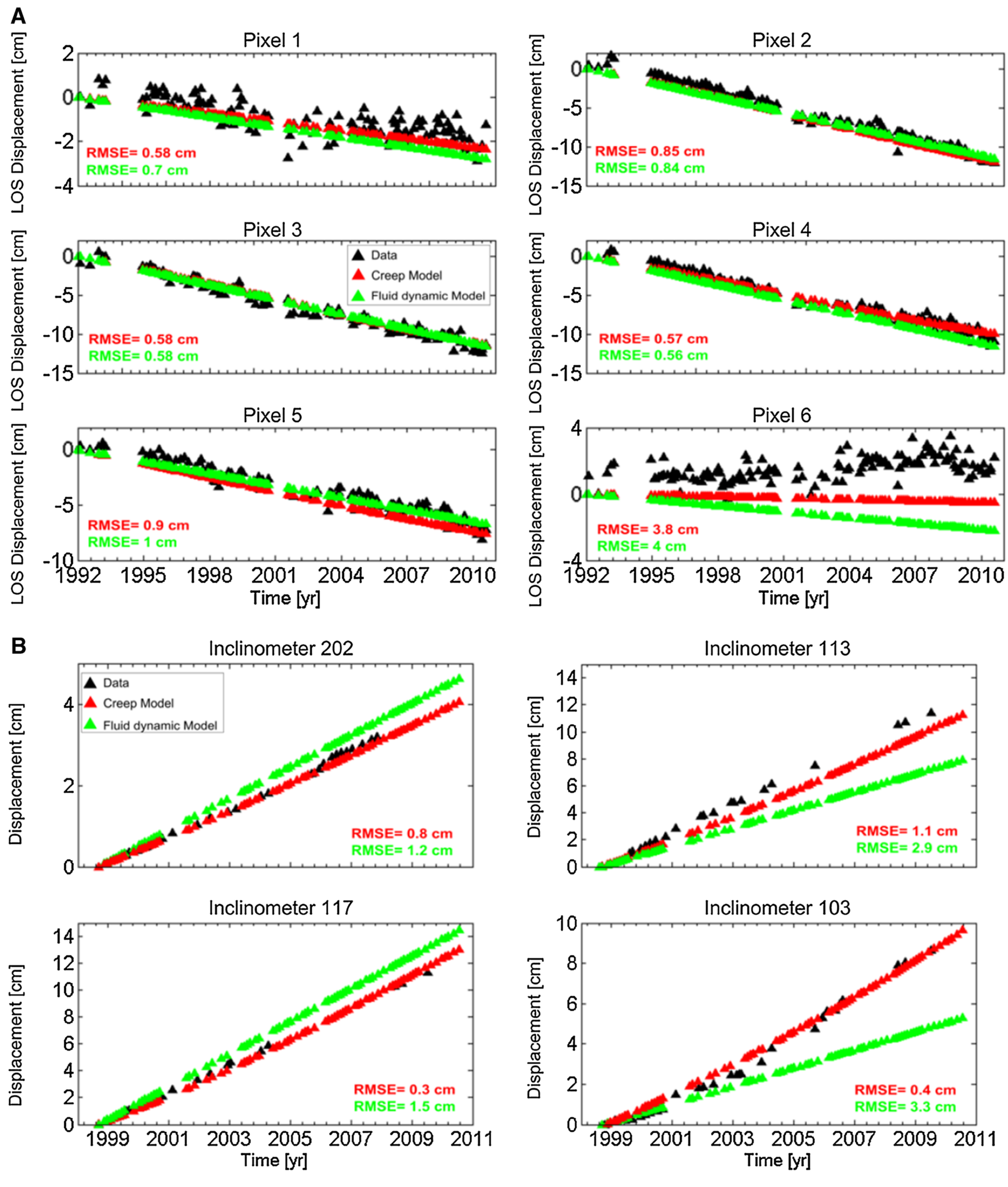

Figure 4
a Comparison between time series of the six selected SAR pixels (*black triangles*), fluid dynamics model (*green triangles*) and creep model (*red triangles*) results. **b** Comparison between time series of four inclinometers (*black triangles*), fluid dynamics model (*green triangles*) and creep model (*red triangles*) results. The RMSE values are also reported

In the second stage (landslide process), the previously calculated stresses are applied to the whole domain, and the two physical approaches, i.e. the fluid dynamics and deviatoric creep models, were alternatively considered to simulate the kinematical trend of the Ivancich landslide during the 1992–2010 time span. Both analyses implicitly assume that the landslide body, delimited by the shear band, is unstable or in a marginal stability condition; this condition has been specifically verified by means of a limit equilibrium calculation that provided a stability factor of the landslide body close to unity. It is worthwhile stressing that, for both approaches, soil is assumed to behave as a single-phase material. This assumption is supported by the available open-pipe piezometric measurements, locally indicating moderate variations of the water level within the landslide debris, and by electric piezometer measurements showing very low variations of the pore water pressure at the depth of the shear band (Sect. 3.1). Accordingly, we can assume that the pore water pressure regime plays a minor role in the landslide evolution process.

5. *Results*

The optimization procedure, based on a GA, was performed by exploiting the long-term SBAS DInSAR results. In particular, we considered the deformation time series of six SAR pixels located within a distance of 25 m from the landslide longitudinal section S–S′ (Fig. 2b). The GA starts by randomly generating ten models, each characterized by viscosity/creep rate values within the lower and upper bounds reported in Table 2. The model providing the best agreement, in terms of the RMSE criterion, with respect to the DInSAR measurements is selected to define the evolution line. Each subsequent generation is then created by considering a narrower range of viscosity/creep rate values centred on the value found in the previous step. This procedure is iterated until 30 generations, for a total number of 300 forward models. Among these, the viscosity/creep rate (Table 2) corresponding to the model that best fits the DInSAR data is chosen as the final parameter value characterizing the soil in the investigated physical process.

The dynamic viscosity values obtained through the optimization procedure are comparable to those obtained in other landslide case studies reported in literature (Di Maio *et al*. 2013; Conte and Troncone 2011; Ter-Stepanian 1975).

Quantitative comparison between the model results, achieved through the above-described optimization procedure, and the DInSAR time series is shown in Fig. 4a for both physical approaches. The figure shows generally good agreement between the DInSAR monitoring data and the model results, except for pixel 6 (Fig. 4a). The discrepancy observed for pixel 6 is supposed to be related to the reduction in LOS distance of the ground surface at the toe of the slope, which is detected by the DInSAR data but is not simulated by the model.

Furthermore, to validate the performed numerical modelling, we exploited the available inclinometer data acquired from 1998 to 2009 in four boreholes located within the landslide deposit (Fig. 1), and compared the model results with such independent in situ measurements (Fig. 4b).

In terms of RMSE, the deviatoric creep model seems to be more suitable, compared with the fluid dynamics model, to describe the kinematical temporal evolution of the Ivancich landslide. This finding is evident by comparing the two modelled time series with the inclinometer ones, particularly in the case of boreholes 103 and 113 (Fig. 4b), for which a slight curvature of the displacement trend is observed. Concerning these two inclinometers, the deviatoric creep approach is capable of simulating the non-linear increase of the displacements over time.

For this physical approach, the modelled distribution of shear stress (τ_{xy}) with respect to lithostatic conditions and of the cumulative displacement over time along the landslide body are reported in Fig. 5a and b, respectively. In particular, Fig. 5b shows that higher displacement rates characterize the central portions of the landslide, whereas significantly lower rates are found in the upper and lower portions of the slope. As a consequence, an increase of of shear stress distribution in the central region of the shear zone is observed (Fig. 5a).

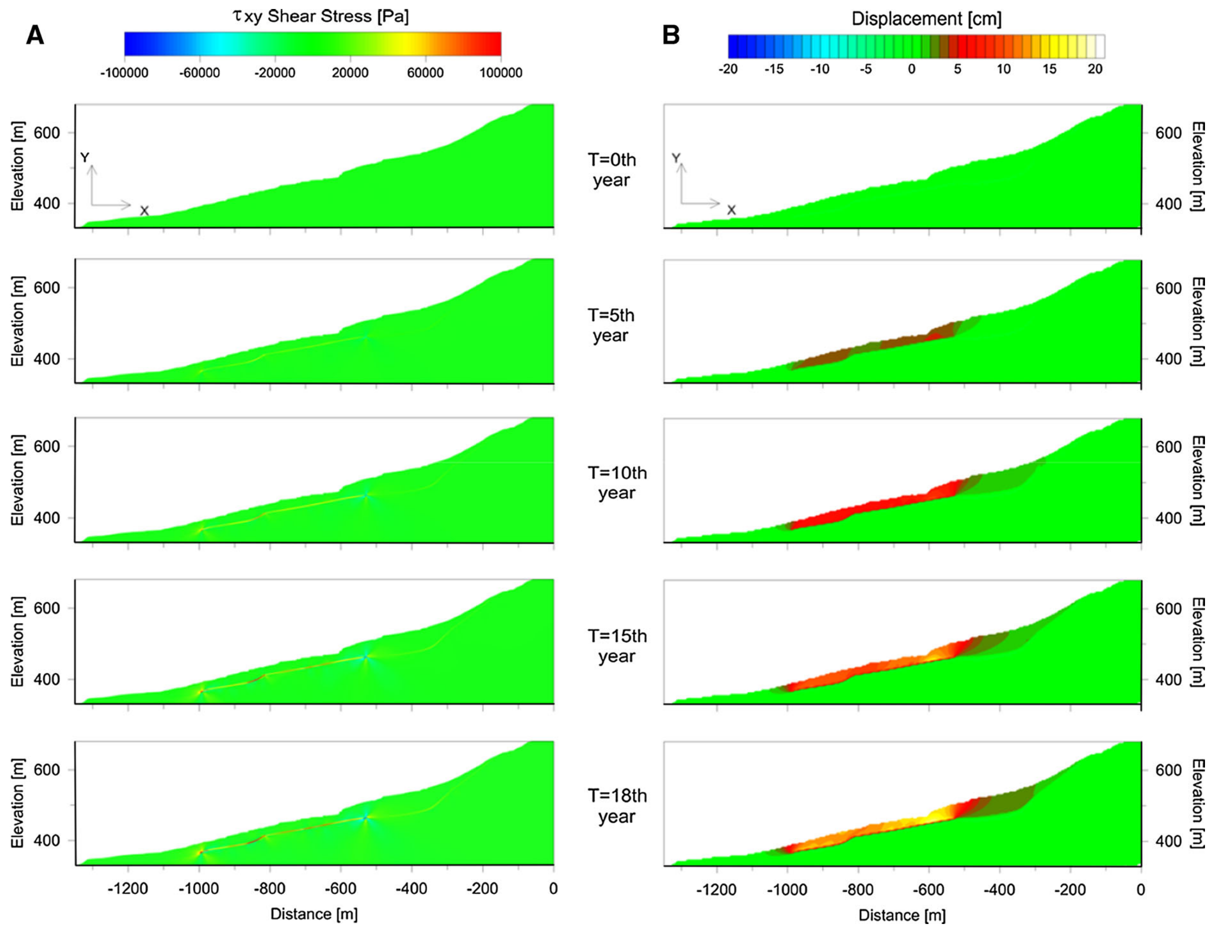

Figure 5

a 2D shear stress and **b** 2D displacement field over time. Both results correspond to the creep numerical simulation

6. Conclusions

In this work, we developed a new procedure to perform inverse numerical modelling of natural phenomena by exploiting DInSAR deformation time series. In particular, we extend the procedure, already proposed in other geoscience contexts such as seismology and volcanology, to investigation of landslide processes.

The proposed methodology is based on integration of the available a priori information, such as geological, geotechnical and geodetic data, into a finite-element environment to build several forward models. By using a Monte Carlo-like optimization procedure, specifically a genetic algorithm, we automatically search for the physical parameter values minimizing the difference between the observed DInSAR deformation time series and modelled displacement field.

The Ivancich landslide (Assisi, central Italy), which is an ancient slow active landslide phenomenon, is considered as a case study. In particular, the kinematical evolution of the unstable mass was analysed by considering a two-dimensional time-dependent FE model using two different physical scenarios, i.e. Newtonian viscous flow and a deviatoric creep model. Quantitative comparison between the results of the two models reveals that, in terms of RMSE (Fig. 4a), the deviatoric creep model is more suitable to describe the temporal evolution of the considered landslide process. This finding is clearly highlighted by comparing the modelled time series with the information derived by inclinometric measurements (Fig. 4b).

Furthermore, based on the optimized creep rate values (Table 2), the highest displacement rates are mainly concentrated in the central regions of the slope, where the minimum values of F_{cr} (1/year) and consequently increase of shear stress are found. Accordingly, the central part of the Ivancich landslide body is supposed to have been active in the last 10,000 years, during the Holocene period. Moreover, analysis of the cumulative displacements points out the presence of an extensional region located near the landslide crown area and a compressive region within the lower area of the landslide body (see $T = 18$th year in Fig. 5b). In this context, the tensile stress region is more enhanced than the compressive one.

Finally, we stress that integration of data derived from geological surveys and remote-sensing and ground-based monitoring measurements within inverse numerical models, through the implementation of optimization procedures, represents a suitable automatic tool to: (i) deeply investigate the kinematical behaviour of slow active landslides in different geological and geomorphological scenarios, and (ii) discriminate the driving forces governing the physical process responsible for the kinematical evolution of the observed phenomenon.

Acknowledgments

Work conducted in the framework of DORIS (Contract no. 242212) and LAMPRE (Contract no. 312384) EC FP7 projects. F. Calò and R. Castaldo were supported by grants of DORIS and LAMPRE projects.

References

Alonso E.E., (2012). Deformation analysis of landslides: progressive failure, rate effects and thermal interactions. Landslides and Engineered Slopes: Protecting society through improved understanding. Eberhardt et al. (eds). Taylor & Francis, London, 175–214.

Angeli M. G., Pontoni, F., (2000). The innovative use of a large diameter microtunneling technique for the deep drainage of a great landslide in an inhabited area: the case of Assisi (Italy). Landslides in research, theory and practice. Thomas Telford, London, 1666–1672.

Angeli M. G., Pontoni, F., (1999). Relazione geologica (Technical Report), 45 pp. (in Italian).

Antonini G., Ardizzone, F., Cacciano, M., Cardinali, M., Castellani, M., Galli, M., Guzzetti, F., Reichenbach, P., Salvati, P., (2002). Rapporto Conclusivo Protocollo d'Intesa fra la Regione dell'Umbria, Direzione Politiche Territoriali Ambiente e Infrastrutture, ed il CNR-IRPI di Perugia per l'acquisizione di nuove informazioni sui fenomeni franosi nella regione dell'Umbria, la realizzazione di una nuova carta inventario dei movimenti franosi e dei siti colpiti da dissesto, l'individuazione e la perimetrazione delle aree a rischio da frana di particolare rilevanza, e l'aggiornamento delle stime sull'incidenza dei fenomeni di dissesto sul tessuto insediativo, infrastrutturale e produttivo regionale. Unpublished Project Report, May 2002, 140 pp (in Italian).

Bagnold *et al*. (1954). *Experiments on a Gravity-Free Dispersion of Large Solid Spheres in a Newtonian Fluid under Shear*, Proc. R. Soc. Lond. A August 6, 1954 *225* 1160 49–63.

Bingul Z., Sekmen A., Zein-Sabatto S., (2000). Evolutionary approach to multi-objective problems using adaptive genetic algorithms, Systems, Man, and Cybernetics, 2000 IEEE International Conference on, pp. 1923–1927, vol. *3*.

Bonano M., Manunta M., Marsella M., Lanari R., (2012). *Long Term ERS/ENVISAT Deformation Time-Series Generation at Full Spatial Resolution via the Extended SBAS Technique*, Int. J. Remote Sens., *33*, 15, pp. 4756–4783, Feb. 2012, doi:10.1080/01431161.2011.638340.

Calò F., Calcaterra, D., Iodice, A., Parise, M., Ramondini, M., (2012). *Assessing the activity of a large landslide in southern Italy by ground-monitoring and SAR interferometric techniques*. International Journal of Remote Sensing, *33*:11, 3512–3530.

Calò F., Ardizzone F., Castaldo R., Lollino P., Tizzani P., Guzzetti F., Lanari R., Angeli M-C., Pontoni F., Manunta M., (2014). *Enhanced landslide investigations through advanced DInSAR techniques: The Ivancich case study, Assisi, Italy*. Remote Sensing of Environment, *142*, pp. 69–82.

Canuti P., Marcucci, E., Trastulli, S., Ventura, P., Vincenti, G., (1986). Studi per la stabilizzazione della frana di Assisi. National Geotechnical Congress, Bologna, 14–16 May 1986, Vol. *1*, 165–174.

Cardinali M., Antonini G., Reichenbach P., Guzzetti, F., (2001). Photo-geological and landslide inventory map for the Upper Tiber River basin. CNR, Gruppo Nazionale per la Difesa dalle Catastrofi Idrogeologiche, Publication n. 2154, scale 1:100,000.

Cascini L., Fornaro G., Peduto D., (2009). *Analysis at medium scale of low-resolution DInSAR data in slow-moving landslide-affected areas*. ISPRS Journal of Photogrammetry and Remote Sensing, *64*, 598–611, doi:10.1016/j.isprsjprs.2009.05.003.

Cascini L., Fornaro G., Peduto D., (2010). *Advanced low- and full-resolution DInSAR map generation for slow-moving landslide analysis at different scales*. Engineering Geology, *112* (1–4), 29–42, doi:10.1016/j.enggeo.2010.01.003.

Chen C.L. and Ling C.H., (1996). *Granular-flow rheology: role of shear-rate number in transition regime*. J. Eng. Mech. ASCE, *122*, No. 5, 469–481.

Conte E. and A. Troncone (2011). *Analytical method for predicting the mobility of slow-moving landslides owing to groundwater fluctuations*. J. Geotech. Geoenv. Eng. ASCE, 777–784.

Crosta G.B., Castellanza R., Frattini, P., Broccolato M., Bertolo, D., Cancelli P., Tamburini A., (2012). Comprehensive understanding of a rapid moving rockslide: the Mt de la Saxe landslide. MIR 2012, Nuovi metodi di indagine monitoraggio e modellazione degli ammassi rocciosi, Barla, G. Ed., Torino, 21–22 novembre 2012, 20 pp.

Cruden D.M., Varnes D.J., (1996). Landslide types and processes. In: Turner, A.K., Schuster, R.L. (eds.) 1996 Landslides, Investigation and Mitigation, Transportation Research Board Special Report 247, Washington, D.C., pp. 36–75.

Di Maio C., Vassallo R., Vallario M. (2013). Plastic and viscous shear displacements of a deep and very slow landslide in stiff clay formation. Engineering Geology, 162, 53–66.

Farina P., Colombo D., Fumagalli A., Marks F., Moretti, S., (2006). *Permanent scatters for landslide investigations: outcomes from the ESA-SLAM project*. Engineering Geology, *88*, 200–217.

Fastellini G., Radicioni F., Stoppini A., (2011). *The Assisi landslide monitoring: a multi-year activity based on geomatic techniques*, Applied Geomatics, 3(2), 91–100, doi:10.1007/s12518-010-0042-9.

Felicioni G., Martini E., Ribaldi C., (1996). Studio dei Centri Abitati Instabili in Umbria. Rubettino Publisher, 418 pp (in Italian).

Gill Ph., Murry W., Wright M., (1981), Practical Optimization. Academic.

Griffiths D. V., Lane P. A., (1999). *Slope stability analysis by finite elements*. Geotechnique *49*, No. 3, 387–403.

Guzzetti F., Manunta M., Ardizzone F., Pepe A., Cardinali M., Zeni G., Reichenbach P., Lanari R., (2009). *Analysis of ground deformation detected using the SBAS-DInSAR technique in Umbria*, *central Italy*. Pure and Applied Geophysics *166*, 1425–1459, doi:10.1007/s00024-009-0491-4.

Hilley G., Bürgmann R., Ferretti A., Novali F., Rocca F., (2004). *Dynamics of slow-moving landslides from permanent scatterer analysis*. Science, 304, 1952–1955, doi:10.1126/science.1098821.

Hunt M.L., Zenit, R., Campbell C.S, Brennen C.E., (2002). *Revisiting the 1954 suspension experiments of R. A. Bagnold*. J. Fluid Mech. 452, 1–24.

Ledesma A., Corominas J., Gonzales DA., Ferrari A., (2009). Modelling slow moving landslide controlled by rainfall. In Picarelli L., Tommasi P., Urciuoli G., Versace P. (eds) Proceedings of the 1st Italian Workshop on Landslides, rainfall-induced Landslides: mechanisms, monitoring techniques and nowcasting models for early warning systems, Naples, 8–10 June 2009, vol. *1*, pp. 196–205.

Leroueil S., (2001). *Natural slopes and cuts: movement and failure mechanisms*. Géotechnique, Volume *51*, Issue 3, pages 197–243.

Lollino, P., Santaloia F., Amorosi A., and Cotecchia F. (2011). *Delayed failure of quarry slopes in stiff clays: The case of the Lucera landslide*. Géotechnique, *61*(10), 861–874.

Manconi A., Tizzani P., Zeni G., Pepe S. and Solaro G., (2009). Simulated Annealing and Genetic Algorithm Optimization using COMSOL Multiphysics: Applications to the Analysis of Ground Deformation in Active Volcanic Areas. Excerpt from the Proceedings of the COMSOL Conference.

Pastor M., Quecedo M., Fernandez-Merodo J.A., Herreros M.I., Gonzalez E., Mira P., (2002). *Modelling tailing dams and mine waste dumps failures*. Geotechnique *52* (8): 579–591.

Perzyna P., (1966). Fundamental Problems in viscoplasticity. Rec. Adv. Appl. Mech. 9, 243–377. Academic, New York.

Pontoni, F., (1999). Unpublished Technical Report, 45 pp (in Italian).

Pontoni, F., (2011). Geoequipe Studio Tecnico Associato Geologia—Ingegneria. Unpublished Technical Report, 4 pp. (in Italian).

Renzhiglov N. F. and T. V. Pavlishcheva, (1970). On the viscosity of rocks. Soviet Mining September–October, 1970, Volume *6*, Issue 5, pp 582–585.

Servizio Geologico Italiano, (1980). Carta Geologica dell'Umbria. Map at 1:250,000 scale (in Italian).

Ter-Stepanian G. (1975). *Creep of a clay during shear and its rheological model*. Géotechnique, *25* (2), 299–320.

Tizzani P., Manconi A., Zeni G., Pepe A., Manzo M., Camacho A., and J. Fernández, (2010). *Long-term versus short-term deformation processes at Tenerife* (*Canary Islands*), J. Geophys. Res., *115*, B12412, doi:10.1029/2010JB007735.

Tizzani P., Castaldo R., Solaro G., Pepe S., Bonano M., Casu F., Manunta M., Manzo M., Pepe A., Samsonov S., Lanari R., Sansosti E., (2013). *New insights into the 2012 Emilia* (*Italy*) *seismic sequence through advanced numerical modeling of ground deformation InSAR measurements*, Geophysical Research Letters, Volume *40*, Issue 10, pages 1971–1977.

Troncone A., (2005). *Numerical analysis of a landslide in soils with strain-softening behaviour*. Géotechnique, *55*(8), 585–596.

Vulliet L., Hutter K. (1988). *Viscous-type sliding laws for landslides*. Canadian Geotechnical Journal, 25, 467–477.

Zhang Z., Zhu J.Z., (1998). *Analysis of the superconvergent patch recovery technique and a posteriori error estimator in the finite element method* (*II*). Comput. Methods Appl. Mech. Eng. *163*, 159–170.

Zienkiewicz O.C., Taylor R.L., (1988). The Finite Element Method: Basic Formulation and Linear Problems, Volume *1*. McGraw-Hill.

(Received March 10, 2014, revised November 22, 2014, accepted December 5, 2014)